

K^-NN absorption and kaonic atoms

Jaroslava Óbertová

*Nuclear Physics Institute, Řež
& FNSPE, CTU in Prague*

Àngels Ramos

University of Barcelona

Eli Friedman

Hebrew University, Jerusalem

Jiří Mareš

Nuclear Physics Institute, Řež

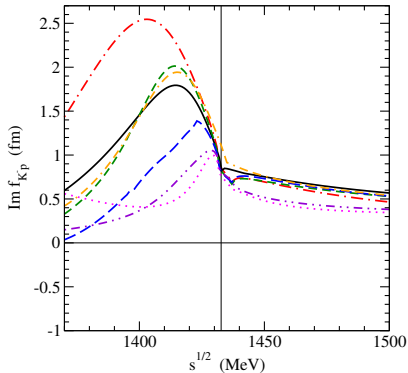
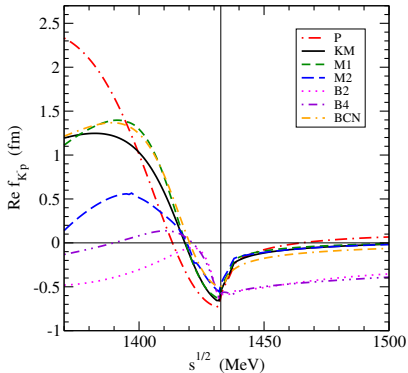
Fundamental Physics at the Strangeness Frontier at DAFNE

25 - 26 February, 2021

Introduction

- K^- multi-nucleon absorption in the surface region of atomic nuclei represents about 20%
NC 53 (1968) 313 (Berkeley), NPB 35 (1971) 332 (BNL), NC 39A (1977) 538 (CERN)
- K^- multi-nucleon absorption in atoms described by phenomenological optical potential
E. Friedman, A. Gal, NPA 959 (2017) 66
- Model for K^-NN absorption in nuclear matter using free-space chiral amplitudes
T. Sekihara et al., PRC 86 (2012) 065205
- New experimental data on K^-NN absorption (AMADEUS@DAΦNE)
K. Piscicchia et al., PLB 782 (2018) 339
R. Del Grande et al., EPJ C79 (2019) 190
- Solid microscopic model for K^-NN absorption needed

Free-space K^-p amplitudes in various chiral models



Prague (P)

Kyoto-Munich (KM)

Murcia (M1 and M2)

Bonn (B2 and B4)

Barcelona (BCN)

A. Cieply, J. Smejkal, *Nucl. Phys. A* 881 (2012) 115

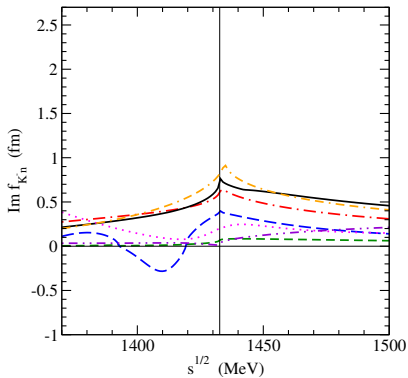
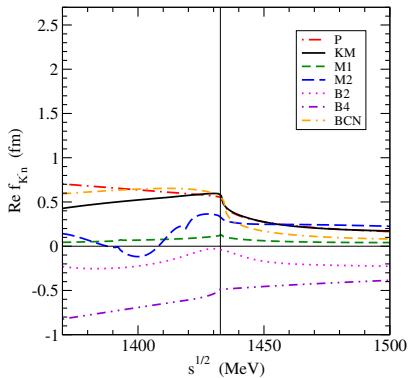
Y. Ikeda, T. Hyodo, W. Weise, *Nucl. Phys. A* 881 (2012) 98

Z. H. Guo, J. A. Oller, *Phys. Rev. C* 87 (2013) 035202

M. Mai, U.-G. Meißner, *Nucl. Phys. A* 900 (2013) 51

A. Feijoo, V. Magas, A. Ramos, *Phys. Rev. C* 99 (2019) 035211

Free-space K^-n amplitudes



Kaonic atoms

- Info about K^-N interaction below threshold provided by kaonic atoms
65 data points (energy shifts, widths, yields=upper level widths)
from CERN, Argonne, RAL, BNL
- Chirally motivated models fail to describe kaonic atom data
E. Friedman, A. Gal, NPA 959 (2017) 66

model	B2	B4	M1	M2	P	KM
$\chi^2(65)$	1174	2358	2544	3548	2300	1806

M multinucleon processes

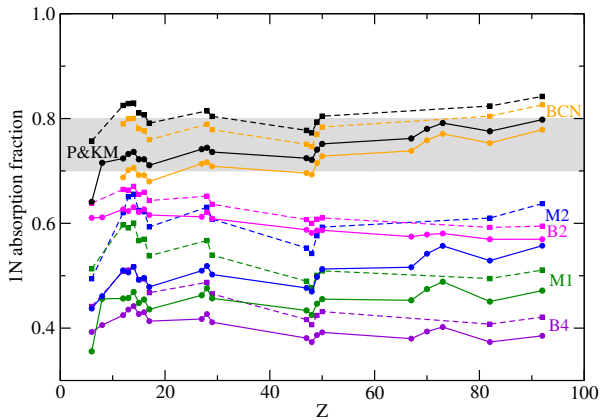
- Chiral models include only $K^- N \rightarrow \pi Y$ ($Y = \Lambda, \Sigma$) decay channel
- K^- interactions with two and more nucleons should be included, (e.g., $K^- + N + N \rightarrow Y + N$) ← analysis of kaonic atom data
E. Friedman, A. Gal, NPA 959 (2017) 66

$$2\text{Re}(\omega_{K^-})V_{K^-}^{(2)} = -4\pi B\left(\frac{\rho}{\rho_0}\right)^\alpha \rho ,$$

where B is a **complex** amplitude, ρ is nuclear density distribution, ρ_0 is saturation density and α is positive

- Amplitude B fitted for each chiral model separately
- $\chi^2(65)$ goes down to 105 - 125

Single- vs. multi-nucleon processes



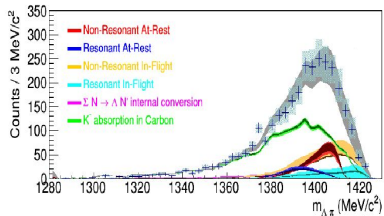
- Fraction of *single-nucleon* absorption 0.75 ± 0.05 (average value) used as an additional constraint.

→ Only P, KM and BCN models found acceptable in kaonic atom analysis
E. Friedman, A. Gal, NPA 959 (2017) 66

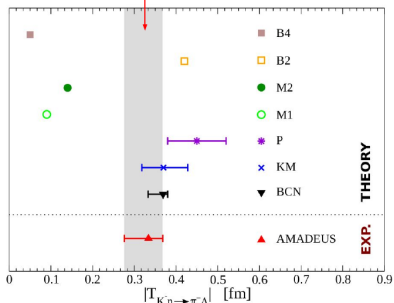
K. Piscicchia, talk at THEIA-STRONG2020 Web-Seminar, 20 December 2020

Outcome of the measurement

Investigated using: $K^- "n" ^3\text{He} \rightarrow \Lambda \pi^- ^3\text{He}$



$$|f_{ar}^s| = (0.334 \pm 0.018 \text{ stat}^{+0.034}_{-0.058} \text{ syst}) \text{ fm.}$$



[K. Piscicchia, S. Wycech, L. Fabbietti et al. Phys.Lett. B782 (2018) 339-345]

[K. Piscicchia, S. Wycech, C. Curceanu, Nucl. Phys. A 954 (2016) 75-93]

Microscopic model for K^-NN absorption in nuclear matter

Microscopic model for K^- two-nucleon absorption in symmetric nuclear matter

J. Hrtáňková, Á. Ramos, PRC 101 (2020) 035204

- based on a meson-exchange approach
H. Nagahiro et al., PLB 709 (2012) 87
- P and BCN chiral K^-N amplitudes employed
- Pauli correlations in the medium for K^-N amplitudes considered
- real part of the K^-NN optical potential evaluated as well
- K^-N optical potential derived within the same approach

K^-N absorption in nuclear matter

$$K^-N \rightarrow \pi Y \quad (Y = \Lambda, \Sigma)$$

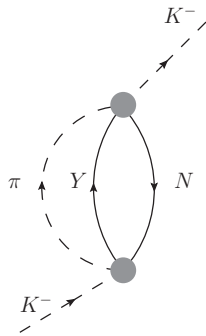
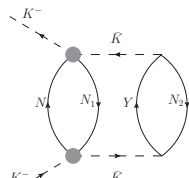
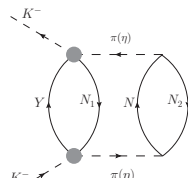


Fig.1: Feynman diagram for K^- absorption on a single nucleon in nuclear matter. The shaded circles denote the K^-N t-matrices derived from a chiral model.

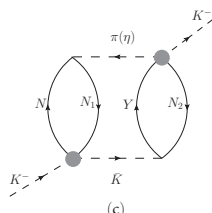
$K^- NN$ absorption in nuclear matter



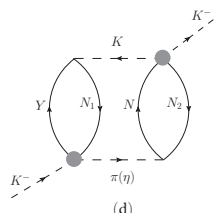
(a)



(b)



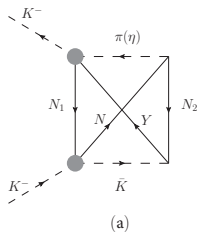
(c)



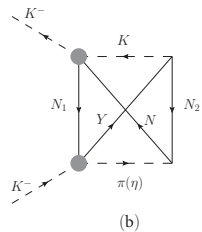
(d)

Fig.2: Two-fermion-loop (2FL) Feynman diagrams for non-mesonic K^- absorption on two nucleons N_1 , N_2 in nuclear matter. The shaded circles denote the K^-N t-matrices derived from a chiral model.

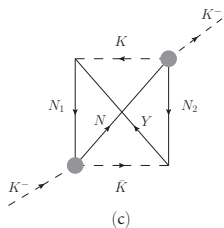
$K^- NN$ absorption in nuclear matter



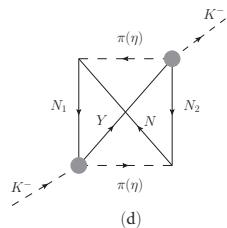
(a)



(b)



(c)



(d)

Fig.3: One-fermion-loop (1FL) Feynman diagrams for non-mesonic K^- absorption on two nucleons N_1 , N_2 in nuclear matter. The shaded circles denote the K^-N t-matrices derived from a chiral model.

$K^- NN$ absorption in nuclear matter

- $V_{K^- N} = \sum_{\text{channels}} V_{K^- N \rightarrow \pi Y}$ (Fig.1)
- $V_{K^- NN} = \sum_{\text{channels}} V_{K^- NN}^{\text{2FL}} + V_{K^- NN}^{\text{1FL}}$ (Fig.2 and 3)
→ contributions from 37 2FL and 28+33 1FL diagrams

Table 1: All considered channels for mesonic and non-mesonic K^- absorption in matter.

$K^- N \rightarrow \pi Y$		$K^- N_1 N_2 \rightarrow Y N$	
$K^- p$	$\rightarrow \pi^0 \Lambda$ $\rightarrow \pi^0 \Sigma^0$ $\rightarrow \pi^+ \Sigma^-$ $\rightarrow \pi^- \Sigma^+$	$K^- pp$	$\rightarrow \Lambda p$ $\rightarrow \Sigma^0 p$ $\rightarrow \Sigma^+ n$
$K^- n$	$\rightarrow \pi^- \Lambda$ $\rightarrow \pi^- \Sigma^0$ $\rightarrow \pi^0 \Sigma^-$	$K^- pn(np)$	$\rightarrow \Lambda n$ $\rightarrow \Sigma^0 n$ $\rightarrow \Sigma^- p$
		$K^- nn$	$\rightarrow \Sigma^- n$

K^- potential in nuclear matter - medium effects

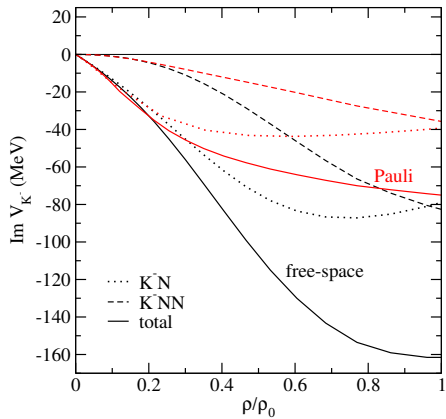
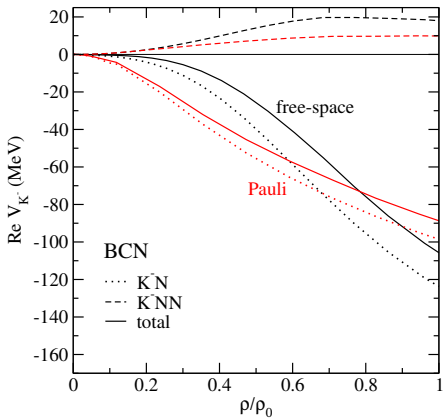


Fig.4: The real (left) and imaginary (right) parts of the $K^- N$, $K^- NN$, and total optical potentials as a function of relative density, calculated using the free-space (black) and Pauli blocked (red) BCN amplitudes for $B_{K^-} = 0$ MeV and $p_{K^-} = 0$ MeV/c.

AMADEUS data

- New measured ratio *R. Del Grande et al., EPJ C79 (2019) 190*

$$R = \frac{\text{BR}(K^- pp \rightarrow \Lambda p)}{\text{BR}(K^- pp \rightarrow \Sigma^0 p)} = 0.7 \pm 0.2(\text{stat.})^{+0.2}_{-0.3}(\text{syst.})$$

- Assumption that dominant contribution for $K^- pp \rightarrow \Lambda p$ and $K^- pp \rightarrow \Sigma^0 p$ channels comes from π^0 exchange leads to relation

$$\frac{\text{BR}(K^- pp \rightarrow \Lambda p)}{\text{BR}(K^- pp \rightarrow \Sigma^0 p)} = \frac{\text{BR}(K^- p \rightarrow \pi^0 \Lambda)}{\text{BR}(K^- p \rightarrow \pi^0 \Sigma^0)}$$

- However, the dominant contribution for $K^- pp \rightarrow \Lambda p$ channel comes from K^- exchange!

T. Sekihara, D. Jido, Y. Kanada-En'yo, PRC 79 (2009) 062201(R)

J. Hrtáková, Á. Ramos, PRC 101 (2020) 035204

Ratio R for 2N absorption

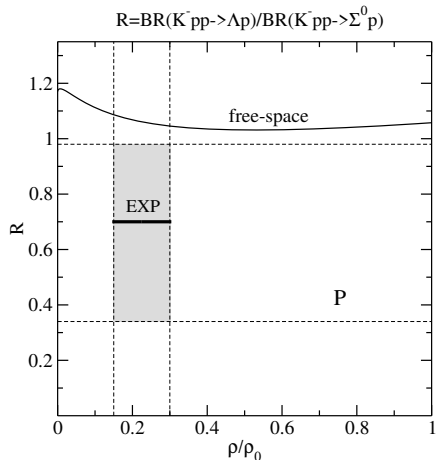
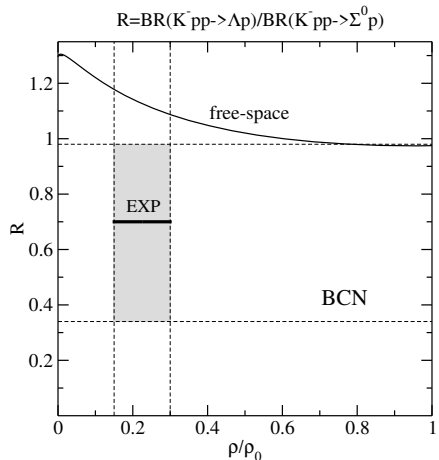


Fig.5: The ratio R as a function of relative density, calculated using the free-space amplitudes for $B_{K^-} = 0$ MeV. The dashed vertical lines denote the region of densities probed in experiments with low-energy K^- including the experimental value of the ratio with corresponding error bar.

Ratio R for $2N$ absorption

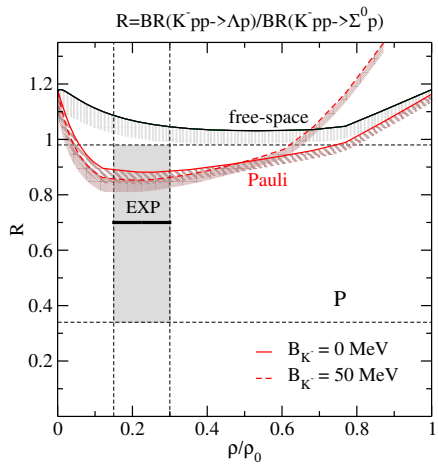
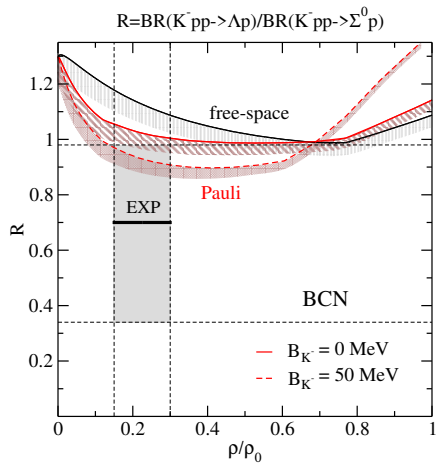


Fig.6: The ratio R as a function of relative density, calculated using the free-space and Pauli blocked amplitudes for $B_{K^-} = 0$ MeV and $B_{K^-} = 50$ MeV. Color bands denote the uncertainty due to different cut-off values $\Lambda_c = 800 - 1200$ MeV.

Ratio R^* for 1N absorption

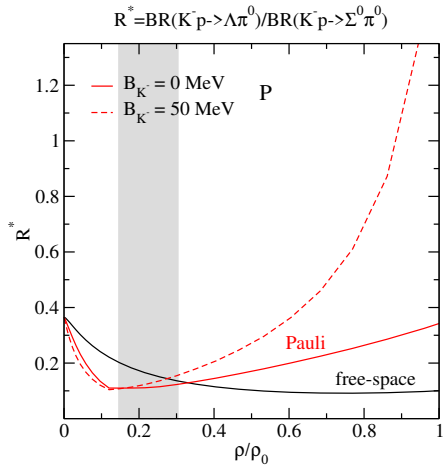
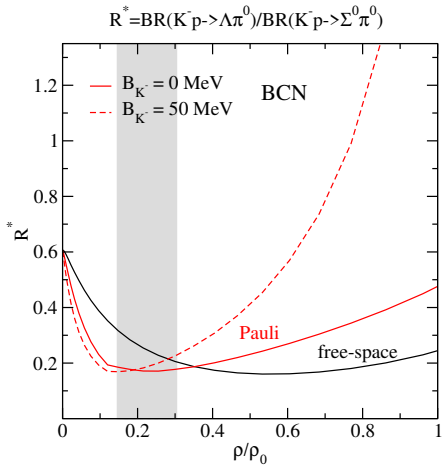


Fig.7: The ratio R^* as a function of relative density, calculated using the free-space and Pauli blocked amplitudes for $B_{K^-} = 0$ MeV and $B_{K^-} = 50$ MeV. The gray band denotes the region of densities probed in experiments with low-energy K^- .

Comparison with experimental data

Table 2: Primary-interaction ratios (in %) for mesonic absorption of K^- in nuclear matter, calculated with free-space and Pauli blocked BCN amplitudes for $B_{K^-} = 0$ MeV $p_{K^-} = 0$ MeV/c. The errors denote the uncertainty due to the cut-off dependence. The experimental data^a are shown for comparison.

BCN mesonic ratio	0.3 ρ_0		Exp. [1]	
	f.s.	Pauli	${}^4\text{He}$	${}^{12}\text{C}$
$\Sigma^+ \pi^- / K^-$	19.6 ± 0.6	28.8 ± 0.7	31.2 ± 5.0	29.4 ± 1.0
$\Sigma^- \pi^0 / K^-$	6.2 ± 0.2	5.7 ± 0.1	4.9 ± 1.3	2.6 ± 0.6
$\Sigma^- \pi^+ / K^-$	21.9 ± 0.6	14.8 ± 0.4	9.1 ± 1.6	13.1 ± 0.4
$\Sigma^0 \pi^- / K^-$	6.2 ± 0.2	5.7 ± 0.1	4.9 ± 1.3	2.6 ± 0.6
$\Sigma^0 \pi^0 / K^-$	18.1 ± 0.5	19.2 ± 0.5	17.7 ± 2.9	20.0 ± 0.7
$\Lambda \pi^0 / K^-$	3.8 ± 0.1	3.5 ± 0.1	5.2 ± 1.6	3.4 ± 0.2
$\Lambda \pi^- / K^-$	7.6 ± 0.2	7.0 ± 0.2	10.5 ± 3.0	6.8 ± 0.3
total 1N ratio	83.3 ± 2.4	84.6 ± 2.2	83.5 ± 7.1	77.9 ± 1.6

^a Corrected for secondary interactions of the primary particles created in the absorbing nucleus.

[1] C. Vander Velde-Wilquet et al., *Nuovo Cimento* 39 A (1977) 538

Comparison with experimental data

Table 3: Primary-interaction total ratios (in %) for non-mesonic and total (1N+2N) K^- absorption in matter and corresponding ratios corrected for Σ - Λ conversion with different conversion rates, a) - 60% for $\Sigma^+ \rightarrow \Lambda$, 22.5% for $\Sigma^- \rightarrow \Lambda$, 72% for $\Sigma^0 \rightarrow \Lambda$, b) - 50% for all Σ 's, calculated with Pauli blocked BCN amplitudes for $B_{K^-} = 0$ MeV. The errors denote the uncertainty due to the cut-off dependence.

BCN	$0.3\rho_0$	$0.3\rho_0 + \Sigma\text{-}\Lambda$ conv.		Exp. [1]
non-mesonic ratio		a)	b)	${}^4\text{He}$
$(\Lambda N + \Sigma^0 N)/K^-$	7.2 ± 1.1	10.5 ± 1.5	11.3 ± 1.6	11.7 ± 2.4
$(\Sigma^- N)/K^-$	4.3 ± 0.6	3.4 ± 0.4	2.2 ± 0.3	3.6 ± 0.9
$\Sigma^+ n/K^-$	3.8 ± 0.5	1.5 ± 0.2	1.9 ± 0.3	1.0 ± 0.4
$(\Sigma^0 N)/K^-$	3.7 ± 0.5	1.0 ± 0.1	1.9 ± 0.2	2.3 ± 1.0
total 2N ratio	15.4 ± 2.2	15.4 ± 2.2		16.4 ± 2.6
total ratio				
Σ^+/K^-	32.6 ± 0.2	13.0 ± 0.1	16.3 ± 0.1	17.0 ± 2.7
Σ^-/K^-	24.8 ± 0.1	19.21 ± 0.04	12.39 ± 0.03	13.8 ± 1.8
Σ^0/K^-	28.7 ± 0.1	8.03 ± 0.04	14.3 ± 0.1	10.8 ± 5.0
Λ/K^-	14.0 ± 0.3	59.7 ± 0.1	57.0 ± 0.2	58.4 ± 5.7
Σ^+/Σ^-	1.31 ± 0.01	0.68 ± 0.01	1.31 ± 0.01	1.2 ± 0.2

Application to kaonic atoms

- K^-NN model applied in calculations of shifts and widths in kaonic atoms
- BCN amplitudes used → in-medium modifications included
(Pauli or WRW) *T. Wass, M. Rho, W. Weise, NPA 617 (1997) 449*
- subthreshold kinematics taken from K^-NN model with
 $p_{K^-} = 150 \text{ MeV/c}$

$$\sqrt{s} = \sqrt{(E_{K^-} + E_F)^2 - \frac{3}{5}k_F^2 - p_{K^-}^2}$$

Kaonic atoms calculations

Table 4: Values of χ^2 for shifts, widths and yields in selected K^- atoms, calculated with K^-N , $K^-N + K^-NN$ and $K^-N+\text{phen}$. multiN potentials based on BCN Pauli or WRW modified amplitudes. Experimental data are shown for comparison.

BCN		WRW		Pauli		phen.	EXP
		KN	+KNN	KN	+KNN	KN + phen.	multiN
C^{12}	$\Delta(\epsilon)$	74.81	20.85	8.46	4.63	0.53	-0.59 (0.08)
	Γ	22.68	21.38	9.46	5.27	1.77	1.73 (0.15)
	Γ^*	1.29	1.17	0.06	0.57	2.45	0.99 (0.20)
P^{31}	$\Delta(\epsilon)$	23.23	6.14	1.84	1.82	0.07	-0.33 (0.08)
	Γ	10.49	12.96	6.02	4.63	0.78	1.44 (0.12)
	Γ^*	7.40	5.96	0.70	0.42	0.42	1.89 (0.30)
S^{32}	$\Delta(\epsilon)$	324.03	134.55	74.54	77.37	15.81	-0.494 (0.038)
	Γ	20.73	40.37	5.35	3.50	0.57	2.19 (0.10)
	Γ^*	37.82	31.30	20.62	14.05	6.47	3.03 (0.44)
Cl^{35}	$\Delta(\epsilon)$	18.81	7.4	0.80	1.15	0.00	-0.99 (0.17)
	Γ	0.26	6.08	3.60	2.70	0.27	2.91 (0.24)
	Γ^*	8.78	5.32	0.60	0.24	0.17	5.8 (1.70)
Cu^{63}	$\Delta(\epsilon)$	9.31	0.43	0.20	0.56	1.23	-0.370 (0.047)
	Γ	0.05	0.46	1.33	1.40	2.23	1.37 (0.17)
	Γ^*	1.39	0.16	0.25	0.47	1.44	5.2 (1.1)
Sn^{118}	$\Delta(\epsilon)$	2.52	2.57	4.71	5.12	3.23	-0.41 (0.18)
	Γ	0.06	0.06	0.06	0.25	0.45	3.18 (0.64)
	Γ^*	22.83	14.44	6.31	5.72	4.09	15.1 (4.4)
Pb^{208}	$\Delta(\epsilon)$	0.12	0.50	0.13	0.41	1.14	-0.02 (0.012)
	Γ	0.09	0.06	0.21	0.29	0.41	0.37 (0.15)
	Γ^*	0.11	0.26	0.39	0.44	0.50	4.1 (2)
χ^2	total	586.82	312.43	145.62	131.01	44.00	
	S^{32}_{out}	204.24	106.20	45.10	36.09	21.16	

Kaonic atom data - ^{32}S

E. Friedman et al, NPA 579 (1994) 518

- $\chi^2(^{32}\text{S})=94.92$ for 'KN+KNN Pauli'
- comparison with data from Ref. [18]:
 - configuration with $2\text{p}+2\text{n}$ in $2\text{s}1/2 \rightarrow \chi^2(^{32}\text{S})=43.15!$
 - configuration with $2\text{p}+2\text{n}$ in $1\text{d}3/2 \rightarrow \chi^2(^{32}\text{S})=26.69!$

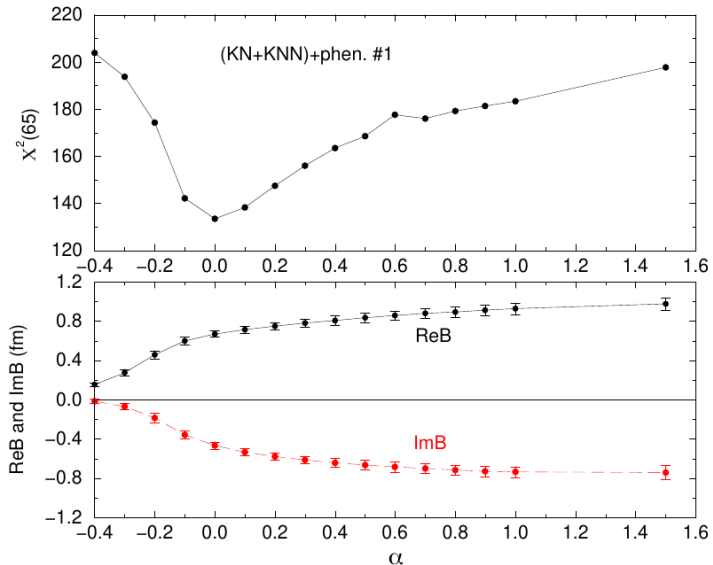
Table 1
Compilation of K^- atomic data

Nucleus	Transition	ϵ (keV)	Γ (keV)	Y	Γ_u (eV)	Ref.
S	$4 \rightarrow 3$	-0.550 ± 0.06	2.330 ± 0.200	0.22 ± 0.02	3.10 ± 0.36	[18]
		-0.43 ± 0.12	2.310 ± 0.170	—	—	[21]
		-0.462 ± 0.054	1.96 ± 0.17	0.23 ± 0.03	2.9 ± 0.5	[19]
Cl	$4 \rightarrow 3$	-0.770 ± 0.40	3.80 ± 1.0	0.16 ± 0.04	5.8 ± 1.7	[18]
		-0.94 ± 0.40	3.92 ± 0.99	—	—	[22]
		-1.08 ± 0.22	2.79 ± 0.25	—	—	[21]
Co	$5 \rightarrow 4$	-0.099 ± 0.106	0.64 ± 0.25	—	—	[19]
Ni	$5 \rightarrow 4$	-0.180 ± 0.070	0.59 ± 0.21	0.30 ± 0.08	5.9 ± 2.3	[20]
		-0.246 ± 0.052	1.23 ± 0.14	—	—	[19]
Cu	$5 \rightarrow 4$	-0.240 ± 0.220	1.650 ± 0.72	0.29 ± 0.11	7.0 ± 3.8	[20]
		-0.377 ± 0.048	1.35 ± 0.17	0.36 ± 0.05	5.1 ± 1.1	[19]

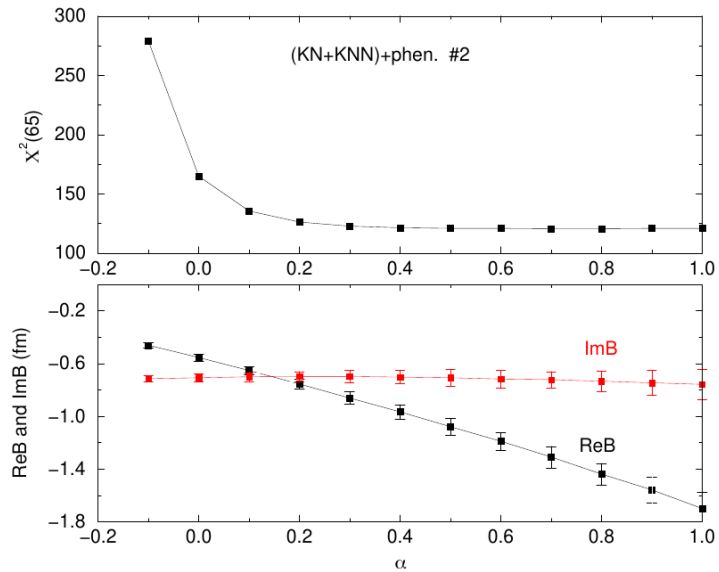
Kaonic atoms calculations

- best χ^2 obtained for $K^-N + \text{mic. } K^-NN$ potentials evaluated using Pauli blocked BCN amplitudes and $p_{K^-} = 150 \text{ MeV/c}$
(other values of p_{K^-} were considered as well)
- these $K^-N + K^-NN$ potentials were calculated for 23 targets and confronted with kaonic atom data $\rightarrow \chi^2(65)=338.2$ (5.20 per point)
- $K^-N + K^-NN$ potentials then supplemented by a phenomenological term describing 3 and 4 nucleon processes $\sim -4\pi B(\frac{\rho}{\rho_0})^\alpha \rho$
- values of α and complex amplitude B fitted to data

Fit to kaonic atom data #1: $\text{Re}B > 0$



Fit to kaonic atom data #2: $\text{Re}B < 0$



Results

- **#1** $\alpha = 0.00 \pm 0.04$, $\text{Re}B = 0.66 \pm 0.04$ fm, $\text{Im}B = -0.46 \pm 0.04$ fm
- **#2** $\alpha > 0.3$, $\text{Re}B$ and $\text{Im}B < 0$
- $K^- N \rightarrow K^- N + K^- NN \rightarrow K^- N + K^- NN + \text{phen. term}$

	$K^- N$	$K^- N + K^- NN$	+ phen.	$K^- N + \text{phen.}$
$\chi^2(65)$	2829	338.2 (286.4*)	133	112.3
$\chi^2/\text{d.p.}$	43.8	5.2 (4.4*)	2.1	1.7

* with data for ${}^{32}\text{S}$ from Ref. [18]

- additional fit with rescaled potential $\beta_{SF}(K^- N + K^- NN) \rightarrow \text{Re}\beta_{SF} = 1.68 \pm 0.027$ and $\text{Im}\beta_{SF} = 0.57 \pm 0.022$ and $\chi^2(65) = 113$

Conclusions: K^-NN model

- Interactions of K^- with two and more nucleons important for realistic description of the K^- -nucleus interaction
- We have developed a microscopic model for K^-NN absorption in nuclear matter using scattering amplitudes derived from the P and BCN chiral meson-baryon interaction models

J. Hrtánková, Á. Ramos, PRC 101 (2020) 035204

- Pauli blocked amplitudes included → medium effects non-negligible
- Calculated ratios in a good agreement with experimental data!

Conclusions: kaonic atoms calculations

- The microscopic K^-NN model was applied in the calculations of kaonic atoms
- Preliminary results:
 - data are best described by $K^-N + K^-NN$ potentials based on Pauli blocked BCN amplitudes
 - $K^-N + K^-NN$ potentials supplemented by a phenomenological term describing 3 and 4 nucleon processes
 - fit to the data suggests that $\text{Re}(K^-N + K^-NN)$ should be more attractive and $\text{Im}(K^-N + K^-NN)$ should be less absorptive
- EXPERIMENT:
 - It would be desirable to revise some kaonic atom data
 - More data on 3N and 4N absorption fractions are needed

What to do next?

- test more values for p_{K^-} ($= 0, 100$ MeV/c, LDA...)
- different approach to \sqrt{s} from studies of kaonic atoms
- confront with data $K^-N + K^-NN$ potentials based on WRW modified amplitudes
- include missing baryon self-energies in in-medium modified amplitudes
- fully self-consistent approach